Photoemission studies of the commensurate-incommensurate transition in the system Xe-Cu(110)

C. Mariani, K. Horn, and A. M. Bradshaw
Fritz-Haber-Institut der Max-Planck-Gesellschaft, D-1000 Berlin 33, Faradayweg 4-6, West Germany
(Received 26 October 1981)

The formation of two-dimensional electronic bands in ordered layers of Xe adsorbed on Cu(110) has been studied with angle-resolved photoemission. The $E(\vec{k}_{||})$ dispersion relation is already measurable for the $c(2\times2)$ layer, as well as for the incommensurate structure formed at higher coverage by a uniaxial compression parallel to the $[1\bar{1}0]$ crystal azimuth. The positions of the surface Brillouin-zone boundaries as determined from band minima agree well with low-energy electron diffraction observations, and the general trends in the band structure are as expected from quasihexagonal layers. The commensurate-incommensurate transition leads to a substantial increase in bandwidth, and causes new photoemission peaks to occur due to multiple scattering at the substrate surface ("substrate umklapp").

I. INTRODUCTION

Lateral interactions among atoms or molecules adsorbed on a solid surface either by direct orbital overlap ("through space") or by interaction of adparticles with the electronic levels of the substrate ("through bond") may lead to a situation in which the valence levels of the adsorbate lose their localized character. When the layer is ordered, a description in terms of two-dimensional Bloch states becomes more appropriate.[1,2] The valence states of the adsorbate are then characterized by the parallel component of electron momentum $\vec{k}_{||}$. These two-dimensional band structures can be measured directly by angle-resolved photoelectron spectroscopy.[3] This is due to the fact that electron momentum parallel to the surface is conserved in the photoemission process, whereas the momentum component $\vec{k}_{\perp}$ is changed because the electron has to cross the potential step at the surface. Such energy bands resulting from interaction among adsorbed species have recently been observed for a variety of adsorption systems, ranging from physisorbed rare-gas atoms to strongly chemisorbed atoms and molecules, on free-electron-like metals, *d*-band metals, and semiconductors.[3–9] Often, only detailed theoretical calculations yield a reasonable description of the observed effects; in principle, the initial as well as final states need to be taken into account, although there are several examples in which a simple tight-binding calculation gives good agreement with experiment[4,5,10] despite the fact that one compares a ground-state calculation with the dispersion of the hole state as measured in the experiment. The agreement between theory and experiment is particularly good for weakly bound adsorbates, for example, the rare gases; since chemical interaction with the substrate can probably be neglected, a consideration of the layer alone often yields satisfactory results.[4,11] It has been shown that this model explains the features observed for xenon on palladium (100), either by using tight-binding methods[10] or a more sophisticated "linear rigorous cellular" (LRC) method.[11] A number of questions were, however, left open in the Xe-Pd(100) experiments. On the Pd(100) surface, the hexagonal xenon overlayer consists of two orthogonal domains. These have only one direction in common, and this does not correspond to a line of high symmetry. Comparison between theory and experiment is therefore impeded; along the lines of high symmetry there are contributions from two domains in the photoelectron spectrum, which in turn lead to a superposition of photoemission peaks.[5]

In order to avoid some of the problems encountered on the fourfold symmetric Pd(100) surface, we have investigated the adsorption of xenon on Cu(110). Here, the twofold symmetry of the surface allows only one domain to form.[12] A more

important feature rendering a study of xenon on Cu(110) worthwhile is, however, the occurrence of a commensurate-incommensurate (*C-I*) phase transition in the layer. At about 90% of the full monolayer a $c(2\times2)$ xenon overlayer exists which is transformed into a nearly hexagonal layer by uniaxial compression along the $[1\bar{1}0]$ aximuth of the Cu(110) substrate; this transition has been recently proposed as a model system for one-dimensional *C-I* phenomena.[13] The study of this phase transition also allows us to unambiguously determine the origin of satellite peaks previously observed on the 5*p* photoemission peaks of adsorbed xenon.[4,5]

II. EXPERIMENTAL

All experiments were carried out in an ultra-high-vacuum photoelectron spectrometer (VG Scientific Ltd., ADES 400) equipped with a rare-gas discharge lamp, a low-energy electron diffraction (LEED) optics, and other ancillary equipment for crystal preparation and gas dosing. The crystals were cut from a single-crystal rod of 5N purity, oriented to within 0.5° of the $[1\bar{1}0]$ direction, and inserted into the vacuum chamber after mechanical and electrolytic polishing. After bake-out, base pressures below 7×10^{-11} Torr were routinely obtained. The crystal was mounted on a manipulator allowing two independent rotations, and could be resistively heated to 900 K and cooled to 20 K by using cold helium gas as the refrigerant.[14] All photoelectron spectra shown were recorded using unpolarized He I radiation ($\hbar\omega=21.2$ eV), with an electron analyzer resolution of 100–180 meV. The crystal was cleaned *in situ* by cycles of argon-ion bombardment and annealing. Absolute work functions could be determined by measuring the total width of the photoelectron spectrum with a potential of −20 V applied to the crystal; changes in work function due to adsorbed gases were measured similarly with an estimated accuracy of ±20 meV.

III. RESULTS AND DISCUSSION

Xenon adsorption on low-index copper single-crystal surfaces was first studied with low-energy electron diffraction (LEED) by Chesters *et al.*[12] They found that at nearly full coverage, a $c(2\times2)$ ordered layer is formed on Cu(110), which transforms into a pseudohexagonal compressed layer as more xenon is adsorbed. This compression occurs along the troughs of the Cu(110) surface, i.e., along the $[1\bar{1}0]$ azimuth. This adsorption system was recently reinvestigated with LEED by Jaubert *et al.*[13] They recorded in detail the transition from the $c(2\times2)$ structure at 90% coverage to the compression at full coverage, determining the distance between adsorbed xenon atoms from LEED patterns for different stages of compression. Due to the limited resolution available in LEED, the region close to the commensurate-incommensurate transition could not be investigated, such that the order of the transition could not be determined; in the region accessible to experiment, the transition seemed to be continuous.[13] They also took isotherm data and calculated the isosteric heat of adsorption for a few coverages. Their study coincides with a recent surge of theoretical interest in *C-I* transitions in two-dimensional systems.[15–18]

In photoemission with He I light, photoelectrons emerging from the Xe 5*p* valence electronic levels are observed in the spectrum. This is shown in Fig. 1 where spectra of the clean and adsorbate-covered surface, taken under otherwise identical conditions, are compared. The lower one is a spectrum of the clean surface, where emission from the copper *d* bands can be clearly observed in the region of the spectrum about 2–5 eV below E_F. The upper spectrum exhibits the extra features due to the adsorption of a monolayer of xenon, namely two strong main peaks around 5.5 to 8 eV below E_F. Photoionization cross sections are extremely high for the Xe 5*p* levels around photon energies of 15–28 eV as compared to other adsorbate valence levels; for xenon on Ni(110) the maximum is close to $\hbar\omega=25$ eV.[17] The high intensity and narrow width of these peaks (FWHM=0.3–0.5 eV) allow

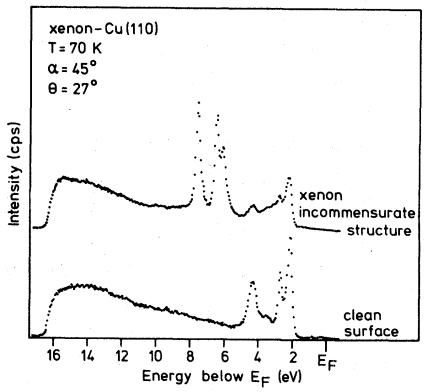

FIG. 1. Photoelectron spectra of a clean and xenon-covered Cu(110) surface, recorded with He I light. Angle of incidence 45°; polar angle of emission $\theta=27°$.

changes in their binding energy to be observed easily. The occurrence of two main emission peaks from xenon arises from the interaction of the spin magnetic moment with the orbital motion of the electron, by which two different levels are produced depending on whether the spin and orbital angular momenta are parallel or antiparallel. This spin-orbit interaction causes the binding energy of the $5p_{1/2}$ state with parallel angular and spin momenta to be lower than that of the $5p_{3/2}$ state with antiparallel momentum vectors. The degeneracy of levels in the free atoms is lowered depending on the geometrical arrangement of the xenon atoms in the layer. This leads to a further splitting of the $5p_{3/2}$ into two components with different magnetic quantum numbers, $m_j = \pm\frac{1}{2}$ and $m_j = \pm\frac{3}{2}$; this is discussed in more detail in Refs. 4 and 5. At normal emission and full coverage the xenon peaks are situated at 7.3 eV ($5p_{1/2}$, $m_j \pm \frac{1}{2}$), 6.1 eV ($5p_{3/2}$, $m_j \pm \frac{1}{2}$), and 5.7 eV ($5p_{3/2}$, $m_j \pm \frac{3}{2}$) below the Fermi energy E_F. This assignment is only valid in normal emission however. This binding energy is usually difficult to compare with the ionization energy of the same levels for the gas-phase species, since relaxation shifts and initial-state shifts may occur. Hulse *et al.*[19] have recently undertaken a comparative study of xenon adsorption on five different metal surfaces, namely Pt, Ir, Ru, Pd, and Cr. Surfaces of several different crystallographic orientations were studied, and from a comparison of Xe $5p_{1/2}$ binding energies and the work functions of the clean metal surfaces it was concluded that a correlation exists between this binding energy and the work function in a particular adsorption environment. The result is that the binding energy of the Xe $5p_{1/2}$ peak with respect to the vacuum level is constant to within 0.2 eV for all surfaces studied. The explanation given by Hulse *et al.* is that the xenon atom is located outside the dipole barrier of the metal surface, and that the initial-state shift is small because of the lack of charge transfer. Thus, the Xe $5p$ levels are pinned to the vacuum level just outside the unoccupied surface site. This effect was used to determine, from the occurrence of several peaks due to the Xe $5p_{1/2}$ level on heterogeneous surfaces, the relative abundance of different crystallographic facets. By adding the binding energy of the Xe $5p_{1/2}$ peak and the work function of the clean surface, one arrives at a binding energy with respect to the vacuum level E_B^V, of 12.3 ± 0.15 eV for all different surfaces. By comparison with the gas-phase value of 13.4 eV this yields a relaxation shift of 1.1 eV which is concluded to be virtually constant for all metal surfaces studied. Note, however, that Kaindl *et al.*,[20] in a synchrotron radiation study of Xe-Pd(100), obtain a value of 1.7 eV for the relaxation shift.

In order to apply the reasoning of Hulse *et al.* to the present case of Xe-Cu(110), we have determined the work function of the clean Cu(110) surface from the width of the photoemission spectrum. We find a value of 4.5 eV in good agreement with 4.48 eV as determined by Gartland *et al.*[21] Adding the binding energy of Xe $5p_{1/2}$ peak of 7.3 eV below E_F a value of 11.8 eV is found for E_B^V. Since all metals studied by Hulse *et al.* have d bands reaching up to the Fermi level, the lower binding energy of xenon on Cu may well be caused by the different relaxation shift that the xenon experiences on copper. If image charge screening is the main mechanism for the relaxation, on the other hand, then Cu being more free-electron-like might be expected to screen more effectively. The same is then true for aluminium where Chiang *et al.*[22] have determined a value of 11.8 eV for E_B^V of the $5p_{1/2}$ peak of adsorbed Xe $5p$ on Al(111); if the analysis of Hulse *et al.*[19] is correct, then both Al(111) and Cu(110) provide a higher relaxation shift.

Adsorbed xenon causes a large work-function decrease on many metal surfaces; its value ranges up to about 1 eV, for example on palladium.[23] On Cu(110), the decrease was found to be 0.61 eV as measured by Horn *et al.*[24] using a Kelvin-probe device. In the present study, we have used the position of the low-energy cutoff in the spectra to determine the work-function change with an estimated accuracy of ± 0.02 eV as a function of xenon exposure. The same value of 0.61 eV was found at full coverage. For each exposure, a photoelectron spectrum at normal emission was also recorded, and the area under the $5p_{1/2}$ and $5p_{3/2}$ peaks was determined separately. The work-function change is plotted as a function of peak area in Fig. 2. Within the uncertainties of the experiment, we note a fairly linear behavior, except for the region near full coverage. Since angle-resolved spectra were recorded for this evaluation, matrix element effects may have influenced the angular distribution of intensities, especially at high coverages, such that the trend in the curve becomes less reliable here; angle-integrated measurements or Auger electron spectra are more suitable for measuring the quantity of adsorbed xenon. Obviously, work-function change versus coverage curves

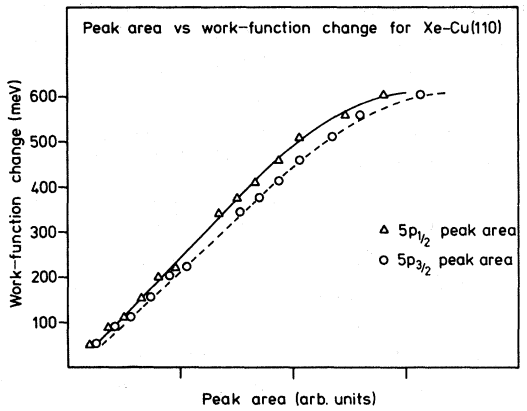

FIG. 2. Peak area of the Xe $5p_{1/2}$ and $5p_{3/2}$ peaks plotted against work-function change for Xe-Cu(110).

need not be linear (and, in general, are not[23]) because of depolarization effects.

The effect of band formation in the adsorbed layer is clearly demonstrated in the set of spectra shown in Fig. 3. Here, the dependence on polar angle of emission-peak energy is shown for the fully compressed layer, the electron emission direction being in the [1$\bar{1}$0] mirror plane of the substrate. The photoemission peaks exhibit a shift in energy with polar angle, with maximum shift amounting to about 0.80 eV. In order to describe the energy shift of the Xe $5p$ levels in terms of two-dimensional bands, structural information about the layer is necessary. For the $c(2\times2)$ layer, the dimensions of the primitive unit cell are readily obtained from the size of the surface unit mesh of the substrate. The size of the unit mesh in the maximum coverage incommensurate layer has been very carefully measured by Jaubert *et al.*[13] From these data, the direct as well as reciprocal lattices for both superstructures have been constructed; they are shown in Fig. 4, along with a diagram of the surface Brillouin zone (SBZ). The distance between xenon atoms long the [1$\bar{1}$0] troughs is 5.10 Å in the $c(2\times2)$ layer and 4.58 Å in the incommensurate layer. Dimensions of the SBZ's are given in Table I.

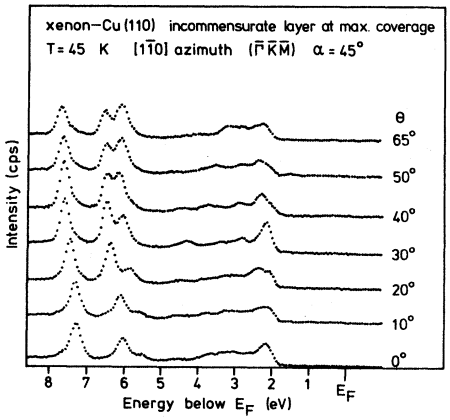

FIG. 3. Series of spectra of an incommensurate xenon layer at maximum coverage for polar angles θ as indicated.

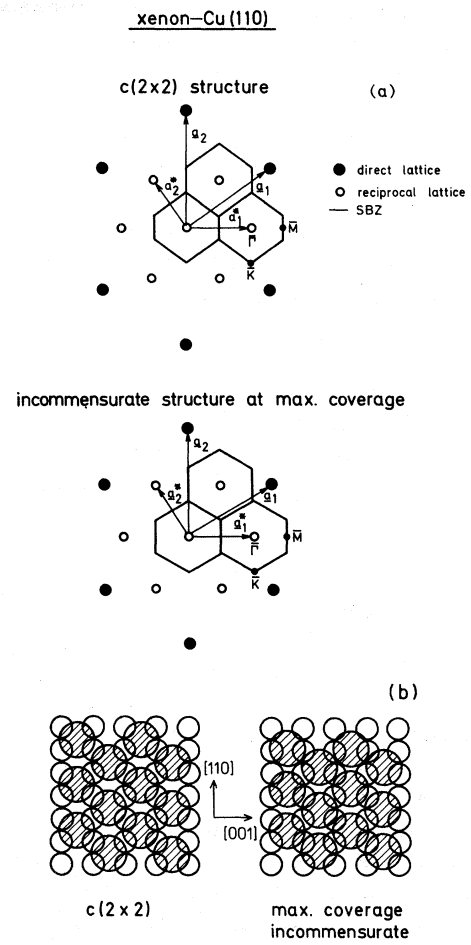

FIG. 4. (a) Representation of the $c(2\times2)$ and maximum coverage incommensurate xenon layers in real and reciprocal space. The first surface Brillouin zone is also indicated. (b) Structure models for both layers in real space.

TABLE I. Dimensions of the surface Brillouin zones for the $c(2\times2)$ and the maximum coverage incommensurate layer for Xe-Cu(110).

	$c(2\times2)$	Incommensurate
$\bar{\Gamma}-\bar{K}$ (Å^{-1})	0.87	0.96
$\bar{\Gamma}-\bar{M}$ (Å^{-1})	0.87	0.87
$\bar{\Gamma}-\bar{K}-\bar{M}$ (Å^{-1})	1.23	1.36
Area per adatom (Å^2)	18.4	16.6

From the isotherm data of Jaubert *et al.* it appears that the transition from the $c(2\times2)$ to the incommensurate layer is accompanied by only a small decrease in the isosteric heat of adsorption. Thus, rather careful control of crystal temperature and equilibrium xenon pressure is necessary in order to establish the $c(2\times2)$ layer below the onset of compression. We were able to record sets of photoelectron spectra for the $c(2\times2)$ as well as for the maximum coverage incommensurate layer. In order to obtain a high degree of accuracy, spectra were recorded for a large number of polar angles which were calculated before the experiment to yield constant differences in $\vec{k}_{||}$ rather than in polar angle. An evaluation of such a sequence of photoelectron spectra, where the parallel photoelectron momentum $\vec{k}_{||}$ was evaluated according to the formula[2]

$$\vec{k}_{||}=\frac{1}{\hbar}(2m_{el}E_{kin})^{1/2}\sin\theta\ , \tag{1}$$

which is shown in Fig. 5 for the $c(2\times2)$ layer. Here we have derived the kinetic energy of the photoelectron by referencing the peak position to the Fermi energy, and by taking work-function and photon energy into account. We observe for the $[1\bar{1}0]$ azimuth that the bands are symmetric around the binding-energy maximum. Along the other azimuth the bands have a maximum near $\vec{k}_{||}=0.85A^{-1}$ and decrease slightly in energy as $\vec{k}_{||}$ is further increased. Considering the shape of the SBZ, we note that the only direction in which the bands are expected to be symmetric is the $\bar{\Gamma}\bar{M}$ direction, which coincides with the [001] crystal azimuth. The shape of the bands is thus as expected from the orientation of the overlayer on the (110) substrate. The $\vec{k}_{||}$ values for the SBZ boundary as evaluated from LEED are given in Table I. We note that the energy of all bands at the $\bar{M}$ point is the same to within 0.1 eV, irrespective of whether we reach it along $\bar{\Gamma}\bar{M}$ or along $\bar{\Gamma}\bar{K}\bar{M}$. This experimental uncertainty of 0.1 eV represents our estimated accuracy for the spectra from the $c(2\times2)$ layer. The photoemission peaks in the $c(2\times2)$ layer recorded at about 75 K are much broader than the spectra from the incommensurate layer, which were recorded at much lower temperature, because the peak width of the xenon valence photoemission peaks exhibits a pronounced temperature dependence.[25] The overall shape of the bands fulfill our expectations for the general trends observed in these bands; in fact, from the shape of the dispersion and a rough knowledge of the size of the SBZ, we can assess which direction corresponds to the $\bar{\Gamma}\bar{M}$ azimuth, since the dispersion curve must be symmetric around the $\bar{M}$ point. Unfortunately, it was not possible to reach the $\bar{\Gamma}$ point of the second SBZ with He I radiation. Making use of Ne II is hindered by the two strong satellite lines present in this discharge line, and for He II ($\hbar\omega=40.8$ eV) the photoionization cross section for the Xe $5p$ levels is too low for recording of spectra in a reasonable amount of time; here the use of synchrotron radiation would be particularly advantageous.

The compression of the xenon overlayer along the $[1\bar{1}0]$ azimuth of Cu(110) leads to pronounced changes in the xenon band structure. This is shown in Fig. 6 where the band structure of the maximum coverage incommensurate layer is de-

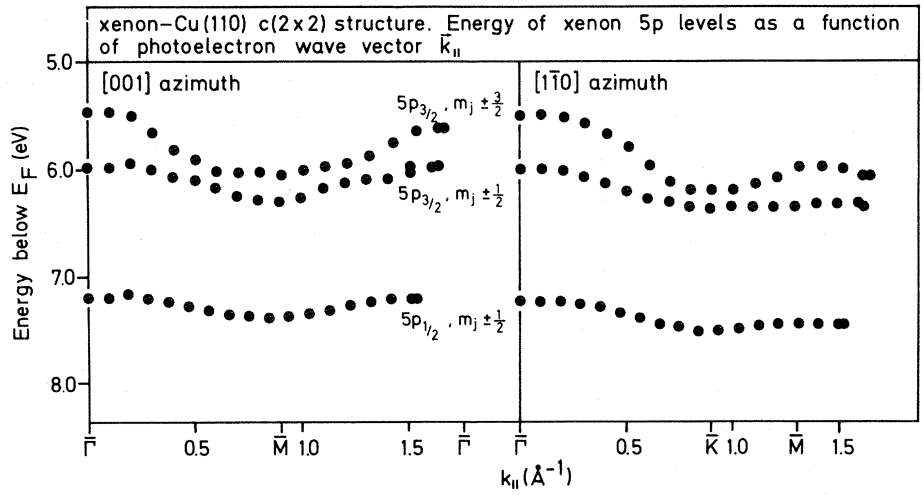

FIG. 5. Experimental band structure of the Xe $5p$ levels in the $c(2\times2)$ layer.

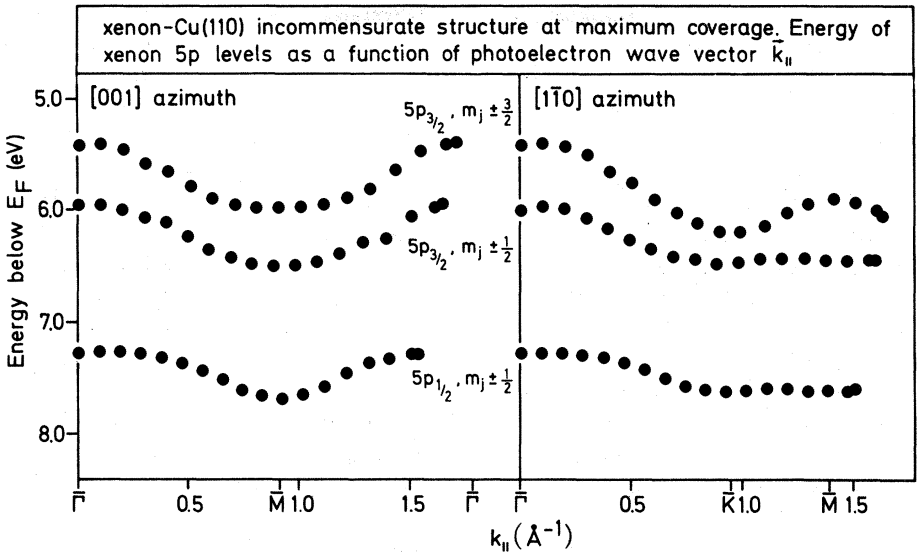

FIG. 6. Experimental band structure of the maximum coverage incommensurate layer.

rived from sets of spectra such as those shown in Figs. 1 and 3 at full coverage. The dispersion widths are increased considerably as is evident from the values given in Table II; a factor of 2 is observed for the $5p_{1/2}$ band with somewhat smaller increases for the other bands. Hermann *et al.*[11] have calculated the dependence of dispersion width on nearest-neighbor distance. They considered a reduction in nearest-neighbor distance of 10% in a hexagonal lattice, which corresponds to a reduction in area per adatom by 17%. By comparison, the area per adatom in going from the $c(2\times2)$ to the fully compressed layer is only reduced by about 10%, so the theoretical values, apart from being evaluated for a hexagonal layer, are expected to be somewhat too large. The calculated increase in bandwidth for the $5p_{1/2}$ band is, however, of the same magnitude as the experimental result. The increase in bandwidth is different for the $\bar{\Gamma}\bar{M}$ and $\bar{\Gamma}\bar{K}$ azimuths. This may reflect the process of uniaxial compression. By close inspection of the band structures presented in Figs. 5 and 6 we observe that the band minima show a slight deviation from the positions of the SBZ boundary as determined by LEED. The magnitude of this difference is of the order of 0.05 to 0.1 Å and is only detected because the energies of the xenon peaks can be determined with high accuracy. The causes for this discrepancy are difficult to determine at present. The band structure as such agrees well with predicted behavior, such that a breakdown of $\vec{k}_{\parallel}$ conservation because of poor ordering in the layer can be ruled out. Relaxation effects may cause the peak to appear at a higher kinetic energy, but this does not affect the shape of the bands as long as $\vec{k}_{\parallel}$ conservation holds. A more intriguing explanation may lie in the actual structure of the overlayer. So far, we have assumed that the structure model on the right side of Fig. 4(b) represents the actual structure of the maximum coverage incommensurate layer. This model does neglect, however, the lateral potential-energy variations on

TABLE II. Bandwidths of the Xe 5*p* valence-level bands in the $c(2\times2)$ and the maximum coverage incommensurate layer, along $\bar{\Gamma}\bar{M}$ and $\bar{\Gamma}\bar{K}$.

Band	$\bar{\Gamma}\bar{M}$		$\bar{\Gamma}\bar{K}$	
	$c(2\times2)$	Incommensurate	$c(2\times2)$	Incommensurate
$5p_{1/2}$	0.20	0.40	0.24	0.40 eV
$5p_{3/2} m_j \pm \frac{1}{2}$	0.36	0.55	0.40	0.60 eV
$5p_{3/2} m_j \pm \frac{3}{2}$	0.40	0.57	0.44	0.80 eV

on the spectra of the $c(2\times2)$ layer, they are connected with the phase transition into the incommensurate structure. Similar peaks have been also observed in photoemission from the hexagonal incommensurate xenon layer on Pd(100) (Refs. 4 and 5) as well as the incommensurate krypton and argon layers on Cu(110).[26] In commensurate layers, the reciprocal-lattice vectors of the adsorbate $\vec{g}_{ads}$ are divisors of the reciprocal-lattice vectors of the substrate $\vec{g}_{sub}$. This means that the formation of the ordered adlayer introduces new (smaller) $\vec{g}$'s, which can lead to a "folding back" of *substrate* emission by a surface umklapp: Owing to scattering at the adlayer in the final state, the parallel component of the electron momentum is conserved with the addition of a reciprocal-lattice vector,

$$\vec{k}_{||_{out}} = \vec{k}_{||_{in}} \pm \vec{g}_{sub} \pm \vec{g}_{ads} \ . \qquad (2)$$

This process was found to account for the changes in the spectrum of the *d*-band region of W(001) upon adsorption of hydrogen in a $c(2\times2)$ structure.[27] The same effect can occur as a result of reconstruction for example in the Si(111)-(2×1) structure.[28] In the case of *photoemission from a commensurate adlayer,* scattering at the substrate in the final state will not lead to such an effect simply because the $\vec{g}_{sub}$ are multiples of the $\vec{g}_{ads}$. In *incommensurate* (including coincidence) layers, however, the $\vec{g}_{ads}$ and $\vec{g}_{sub}$ form completely different sets, hence scattering of a photoelectron off the substrate will give rise to new "photoemission beams" similar to the multiple-scattering beams observed in LEED from incommensurate overlayers. This means that, at a particular polar angle θ, we can observe both photoelectrons directly according to Eq. (1), and photoelectrons originating from different regions of the adsorbate Brillouin zone and subsequently scattered by the substrate. Since the latter generally have a different initial energy, they will appear as additional peaks or shoulders in the spectrum. This variant of surface umklapp, which is different from the case of hydrogen on W(001) in that electrons originating in the adlayer and backscattered from the substrate are involved, is illustrated schematically for the one-dimensional case in Fig. 8(a). In process *A* only equivalent states in the Brillouin zone are involved. Process *B*, in which scattering takes place with the addition or subtraction of a substrate reciprocal-lattice vector, leads to emission of electrons from nonequivalent points for the BZ. Figure 8(b) shows the result of the two processes on the appearance of the photoelectron spectrum from a dispersing level. This illustration approximates the situation where spectra from the incommensurate xenon layer are recorded along the $[1\bar{1}0]$ azimuth, since overlayer and substrate are out of registry only along this direction. The occurrence of the satellite peak in Fig. 7(b) (spectrum of the incommensurate layer) proves that this process is operational here. For a layer out of registry on both high-symmetry azimuths, many more substrate umklapp processes are possible, such that more points in the SBZ contribute to the shoulder peak. The intensity of this shoulder peak will give us an estimate of the fraction of photoelectrons that undergo umklapp scattering at the substrate surface; an evaluation of the spectra presented in Fig. 7 puts their number at about 15% of the directly emitted electrons. By observing the appearance of shoulder peaks such as shown in Fig. 7, we have a means of detecting incommensurate phases even at low coverages where they cannot be distinguished in LEED; a compressed phase does, in fact, occur at low temperatures and low coverages for xenon on Cu(110).[18]

IV. CONCLUSION

The structure of the electronic bands formed by the xenon valence levels in ordered layers on Cu(110) has been determined in angle-resolved photoemission; positions of band minima and max-

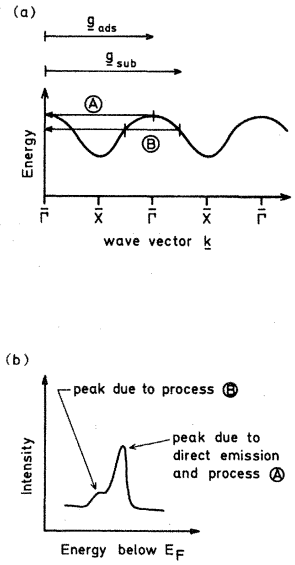

FIG. 8. (a) Schematic illustration of the umklapp processes in an incommensurate layer in a one-dimensional example. (b) Contributions from the umklapp processes to the photoelectron spectrum.

TABLE III. Separation $\Delta\epsilon$ of bands at the $\bar{\Gamma}$ point in the $c(2\times2)$ and the maximum coverage incommensurate layer.

	$c(2\times2)$	Incommensurate	Calc.
$\Delta\epsilon_1$ $(5p_{1/2}/5p_{3/2}m_j\pm\frac{1}{2})$	1.24	1.35	1.32
$\Delta\epsilon_2$ $(5p_{3/2},m_j\pm\frac{1}{2}/5p_{3/2}m_j\pm\frac{3}{2})$	0.44	0.57	0.44

the surface, which lead to the occurrence of modulated surface structures.[13] These may account for the above effects in two-dimensional band structures. The distance of the $\bar{K}$ point from $\bar{\Gamma}$ is increased by some 10% in going from the $c(2\times2)$ to the fully compressed layer (Table I). We thus expect the band minimum to shift to higher $\vec{k}_{||}$ values for the compressed structure. An indication of this effect is given in the lowest binding-energy band of both structures. The band minimum clearly lies nearest to the $\bar{\Gamma}$ point for the $c(2\times2)$ layer. There are situations in which a determination of distances in a layer is not feasible in LEED, either because a (1×1) overlayer is formed, e.g., for hydrogen on some metal surfaces, or when island growth occurs and the coverage is too low such that the overlayer LEED beams are too weak. The latter situation is of interest for a determination of the layer geometry when island growth occurs. Thus, the use of band structures derived from angle-resolved photoemission could also be an important tool in geometrical structure determination.

The separations of the three bands at $\bar{\Gamma}$, i.e., for normal emission, are given in Table III. The values for $\Delta\epsilon_1$, the separation between the $5p_{1/2}$ and the $5p_{3/2}$ $m_j\pm\frac{1}{2}$ band, and $\Delta\epsilon_2$, the separation between the two $5p_{3/2}$ bands, are close to those calculated by Hermann *et al.*[11] As the layer is compressed, the band separation is found to increase by small amounts; the calculated increase (for a comparison by 17%) is somewhat too large.

Are there any other effects apart from the increase in dispersion width which the commensurate-incommensurate transition produces in the photoelectron spectra? In order to answer this question, consider sets of spectra recorded at the same polar angle for the $c(2\times2)$ and the compressed layer. These are shown in Fig. 7. Here, a linear background was subtracted from the spectra in the Xe $5p$ emission region in order to fit the peaks by means of a Gaussian curve-resolving routine. The spectra of the $c(2\times2)$ layer could be adequately represented by three Gaussians of equal half-width, corresponding to the three xenon emission peaks (top spectrum in Fig. 7). When the same analysis is applied to the spectra of the compressed layer, we find that there are additional shoulder peaks which are not represented by the sum of the three Gaussian peaks. (In the lower spectrum, Gaussians of lower half-width were used since these data were taken at much lower temperature, where the peaks are narrower.[25] At normal emission, the shoulders appear on the high-binding-energy side of the main peaks (bottom spectrum of Fig. 7); for $\vec{k}_{||}$ values near the boundary of the SBZ they appear at the low-binding-energy side. Since these shoulders do not appear

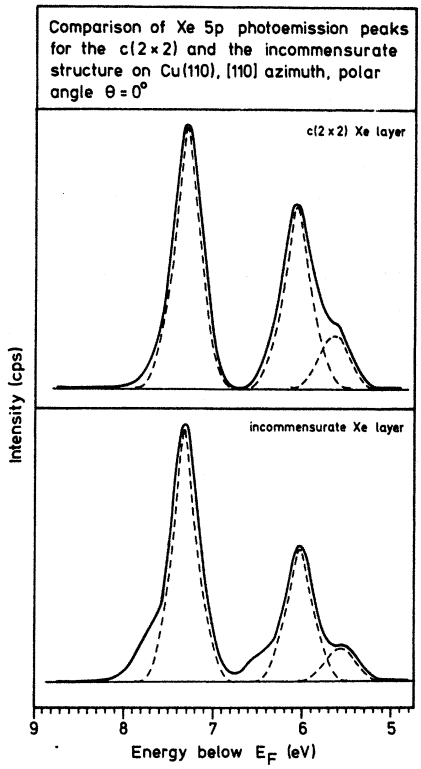

FIG. 7. Comparison of Xe $5p$ photoemission peaks in the $c(2\times2)$ and compressed layers. Note the high-binding-energy shoulders that appear in the spectrum of the incommensurate layer.

ima agree well with the magnitude of the SBZ as derived from LEED for both the commensurate and incommensurate layers. The general appearance of the bands corresponds to the expected course of the dispersion curves. The large increase in bandwidth upon completion of the first monolayer emphasizes the strong dependence on nearest-neighbor distance of band formation in such two-dimensional systems. Thus, xenon on Cu(110) turns out to be a fine example for the importance of the electronic interaction in two-dimensionally ordered systems. The occurrence of peaks due to scattering of the photoelectron at the substrate surface-substrate umklapp gives direct evidence of the mismatch between surface and adlayer unit mesh, i.e., the onset of the formation of an incommensurate phase.

ACKNOWLEDGMENT

This work was supported by the Deutsche Forschungsgemeinschaft through Sonderforschungsbereich 6.

[1]A. Liebsch, Phys. Rev. B 17, 1653 (1978).
[2]A. M. Bradshaw, M. Scheffler, J. Vac. Sci. Technol. 16, 447 (1979).
[3]P. K. Larsen, N. V. Smith, M. Schlüter, H. H. Farrell, K. M. Ho, and M. L. Cohen, Phys. Rev. B 17, 2612 (1978).
[4]K. Horn, M. Scheffler, and A. M. Bradshaw, Phys. Rev. Lett. 41, 822 (1978).
[5]M. Scheffler, K. Horn, A. M. Bradshaw, and K. Kambe, Surf. Sci. 80, 69 (1979).
[6]K. Jacobi and C. V. Muschwitz, Solid State Commun. 26, 477 (1978).
[7]P. Hofmann, C. V. Muschwitz, K. Horn, K. Jacobi, A. M. Bradshaw, K. Kambe, and M. Scheffler, Surf. Sci. 89, 327 (1980).
[8]P. J. Feibelman, D. R. Hamann, and F. J. Himpsel, Phys. Rev. B 22, 1734 (1980).
[9]K. Horn, A. M. Bradshaw, K. Hermann, and I. P. Batra, Solid State Commun. 31, 257 (1979).
[10]K. Kambe, Surf. Sci. 102, 95 (1981).
[11]K. Hermann, J. Noffke, and K. Horn, Phys. Rev. B 22, 1022 (1980).
[12]M. Chesters, M. Hussain, and J. Pritchard, Surf. Sci. 35, 161 (1973).
[13]M. Jaubert, A. Glachant, M. Bienfait, and G. Boato, Phys. Rev. Lett. 46, 1979 (1981).
[14]R. Unwin, K. Horn, and P. Geng, Vakuum-Technik 29, 149 (1980).
[15]J. A. Venables and P. S. Schabes-Retchkiman, J. Phys. (Paris) 38, 105 (1977).
[16]P. W. Stephens, P. Heiney, R. J. Birgeneau, and P. M. Horn, Phys. Rev. Lett. 43, 47 (1979).
[17]R. J. Birgeneau, E. M. Hammons, P. Heiney, P. W. Stephens, and P. M. Horn, in *Ordering in Two Dimensions,* edited by S. K. Sinha (North-Holland, New York, 1980).
[18]K. Horn and C. Mariani (unpublished).
[19]J. Hulse, J. Küppers, K. Wandelt, and G. Ertl, Appl. Surf. Sci. 6, 453 (1980).
[20]G. Kaindl, T. C. Chiang, F. J. Himpsel, and D. E. Eastman, Phys. Rev. Lett. 45, 1808 (1980).
[21]P. O. Gartland, G. Berge, and B. J. Slagsvold, Phys. Rev. Lett. 28, 798 (1972).
[22]T. C. Chiang, G. Kaindl, and D. E. Eastman, Solid State Commun. 36, 25 (1980) and (unpublished).
[23]P. W. Palmberg, Surf. Sci. 28, 25 (1971).
[24]K. Horn, M. Hussain, and J. Pritchard, Surf. Sci. 63, 244 (1977).
[25]J. W. Gadzuk, S. Holloway, C. Mariani, and K. Horn, (unpublished).
[26]K. Horn, C. Mariani, and L. Cramer, (unpublished).
[27]J. Anderson and G. J. Lapeyre, Phys. Rev. Lett. 36, 376 (1976).
[28]F. J. Himpsel, P. Heimann, D. E. Eastman, Phys. Rev. B 24, 2003 (1981).